Unexpected spin-parity assignments of the excited states in ^{9}Be

Y. Hirayama,[1,][*] T. Shimoda,[2] H. Miyatake,[1] H. Izumi,[2] A. Hatakeyama,[3] K. P. Jackson,[4] C. D. P. Levy,[4] M. Pearson,[4] M. Yagi,[2] and H. Yano[2]

[1]*Institute of Particle and Nuclear Studies (IPNS), High Energy Accelerator Research Organization (KEK), Ibaraki 305-0801, Japan*
[2]*Department of Physics, Osaka University, Osaka 560-0043, Japan*
[3]*Institute of Physics, Graduate School of Arts and Sciences, University of Tokyo, Tokyo 153-8902, Japan*
[4]*TRIUMF, 4004 Wesbrook Mall, Vancouver, British Columbia, Canada V6T 2A3*

The excited states in the light nucleus ^{9}Be are studied through β-delayed neutron decays from spin-polarized ^{9}Li$_{\rm g.s.}$. The neutron transitions via ^{5}He$_{\rm g.s.}$ from the 2.43-, 2.78-, 4.704-, 5.59-, and 7.94-MeV states in ^{9}Be are observed for the first time, and the spins and parities (I^π's) of the excited states in ^{9}Be are assigned from β-n coincidences and measurements of the β-decay asymmetries. The spin parity, I^π, of the 2.43-MeV state is assigned to be $5/2^-$, which is consistent with the reported value. The present results suggest that the I^π values of the 2.78-, 4.704-, 5.59-, and 7.94-MeV states are $3/2^-$, $1/2^-$, $5/2^-$, and $3/2^-$, respectively, which are different from early reported values. However, shell-model calculations of the p shell are in overall good agreement with the present results, except for the I^π values of the 2.78- and 4.704-MeV states.

I. INTRODUCTION

The structures of the excited states in ^{9}Be have been repeatedly studied for about 50 yr both experimentally [1–18] and theoretically [19–23] owing to the uncertainties in the decay channels and the spin-parity values of the excited states. Because all the excited states in ^{9}Be (one neutron separation energy $S_n = 1.6653$ MeV [24]) are reported to be unbound states, in spite of the stable nucleus, and have a broad natural width of about 1 MeV, except for the 2.43-MeV state [24], there are experimental difficulties in detecting low-energy neutron and/or α-particle decays. The excited states decay to three particles $\alpha + \alpha + n$ through the following two-body or three-body decay channels:

(i) ^{8}Be(g.s., $\Gamma = 6.8$ eV, $I^\pi = 0^+$) + n
$\rightarrow \alpha + \alpha + n + Q_\alpha$ (=91.84 keV);
(ii) ^{8}Be($E_{\rm x} = 3.04$ MeV, $\Gamma = 1.5$ MeV, $I^\pi = 2^+$) + n
$\rightarrow \alpha + \alpha + n$;
(iii) ^{5}He(g.s., $\Gamma = 0.6$ MeV, $I^\pi = 3/2^-$) + α
$\rightarrow \alpha + \alpha + n + Q_{\rm n}$ (=890 keV);
(iv) ^{5}He($E_{\rm x} = 4.0$ MeV, $\Gamma = 4$ MeV, $I^\pi = 1/2^-$) + α
$\rightarrow \alpha + \alpha + n$;
(v) direct breakup channel $\alpha + \alpha + n$.

The broad natural widths of the ^{5}He and ^{8}Be nuclei also make it difficult to study the structure of the excited states in ^{9}Be.

In the latest compilation [24] by Tilley *et al.*, 12 excited states in ^{9}Be (listed in Table I) to which the ^{9}Li$_{\rm g.s.}$ ($I^\pi = 3/2^-$, $T_{1/2} = 178$ ms, $Q_\beta = 13.6$ MeV [24]) nucleus is energetically able to decay by β decay are reported. Four positive-parity states of $E_{\rm x} = 1.684$, 3.049, 4.704, and 6.76 MeV with $I^\pi = 1/2^+$, $5/2^+$, $(3/2)^+$, and $9/2^+$, respectively, are reported in the compilation. From photo-neutron angular-distribution

measurements [1], the values of I^π of the 1.684-, 3.049-, and 4.704-MeV states have been proposed to be $1/2^+$, $5/2^+$, and $(3/2$ or $5/2)^+$, respectively, by assuming that the states decay to ^{8}Be$_{\rm g.s.}$ ($I^\pi = 0^+$), ^{8}Be$_{\rm g.s.}$, and ^{8}Be$^*(2^+)$ by emitting s-, d-, and s-wave neutrons, respectively. However, in the case of the neutron decay of the 4.704-MeV state, there are two conflicting reports [1,7]. There is ambiguity in the spin-parity assignment for the 4.704-MeV state. The value of $I^\pi = 9/2^+$ for the 6.76-MeV state was suggested based on electron-scattering [11] and proton-scattering experiments [12].

Eight negative-parity states of $E_{\rm x} = 0$, 2.429, 2.78, 5.59, 6.38, 7.94, 11.283, and 11.81 MeV with $I^\pi = 3/2^-$, $5/2^-$, $1/2^-$, $(3/2^-)$, $7/2^-$, $(5/2^-)$, $(7/2^-)$, and $5/2^-$, respectively, are reported in the compilation. The six negative-parity states of 0, 2.43, 2.78, 5.59, 7.94, and 11.81 MeV are populated by an allowed β transition from the ^{9}Li nucleus [24]. Extensive β-decay spectroscopy of ^{9}Li$_{\rm g.s.}$ has been performed for the study of the low-lying states with negative parity in ^{9}Be by measuring β-delayed neutrons [5,6,10] and α particles [9,10,13–15].

The values of I^π of the ground and 2.43-MeV states in ^{9}Be were firmly assigned to be $3/2^-$ and $5/2^-$, respectively, confirmed by several experiments [24]. In the case of the 2.78 ± 0.12-MeV [$I^\pi = 1/2^-$, $\Gamma = 1.08(11)$-MeV] state, there has been no firm spin assignment from β-decay and reaction experiments. According to the predictions of theoretical calculations [19,20,25], the 2.78-MeV state was concluded to be the "missing" $1/2^-$ state. The spin-parity value has been assumed for about 40 yr. Prezado and Borge *et al.* [14,15] deduced the spin-parity value to be $1/2^-$ experimentally from the measurement of the angular correlation of β-delayed α particles. The 5.59(10)-MeV [$I^\pi = (3/2^-)$, $\Gamma = 1.33(36)$] and 6.38(60)-MeV [$I^\pi = 7/2^-$, $\Gamma = 1.21(23)$] states were discovered by Dixit *et al.* [12]. I^π of the 7.94-MeV state was reported to be $(1/2)^-$ in the previous compilation [26], but is reported to be $(5/2)^-$ in the most recent compilation, as suggested by an unpublished thesis [27]. $I^\pi = (7/2^-)$ for the 11.283-MeV state was suggested based on analog evidence

*yoshikazu.hirayama@kek.jp

TABLE I. Excited states in ^{9}Be reported in the latest compilation [24] to which the ^{9}Li$_{g.s.}$ energetically enables transit by β decay, and the states of ^{8}Be and ^{5}He [35]. The values of E_x, Γ, and I^π were considered in the present analysis for the neutron TOF and asymmetry spectra.

Isotope	E_x (MeV)	Γ (keV)	I^π
^{9}Be	1.684(7)	217(10)	$1/2^+$
	2.4294(13)	0.78(13)	$5/2^-$
	2.78(12)	1080(110)	$1/2^-$
	3.049(9)	282(11)	$5/2^+$
	4.704(25)	743(55)	$(3/2)^+$
	5.59(10)	1330(360)	$(3/2)^-$
	6.38(6)	1210(230)	$7/2^-$
	6.76(6)	1330(90)	$9/2^+$
	7.94(8)	≈ 1000	$(5/2)^-$
	11.283(24)	575(50)	$(7/2)^-$
	11.81(2)	400(30)	$5/2^-$
^{8}Be	0.0	6.8×10^{-3}	0^+
	3.04	1500	2^+
^{5}He	0.0	600	$3/2^-$
	4.00	4000	$1/2^-$

of ^{9}B [26]. However, (e,e') [11] and (p,p') [12] experiments suggested a positive parity of $I^\pi = (7/2)^+$. Recently, Prezado and Borge *et al.* [14] assigned $I^\pi = 5/2^-$ for the 11.81-MeV state from the α-α angular distribution measurement.

As mentioned above, it seems that the values of I^π of the excited states in ^{9}Be have not been determined definitely in experiment, except for the ground and 1.684-, 2.429-, 3.049-, and 6.38-MeV states. We investigated β-delayed neutron decays and assigned the spin-parity values of the excited states by different experimental methods, and we investigated the decay channels of the excited states through the decays ^{9}Li$_{g.s.}$(spin-polarized) $\xrightarrow{\beta}$ ^{9}Be* $\xrightarrow{n}$ ^{8}Be and ^{9}Be* $\xrightarrow{n}$ ^{5}He $+\alpha(\rightarrow n + \alpha + \alpha)$. The present experiment is based on the method [28–31] of β-delayed decay spectroscopy using a spin-polarized parent nucleus. Taking advantage of the β-decay asymmetry parameter, which is governed by the spin-parity values of parent and daughter nuclei, the spin-parity value of an excited state in a daughter nucleus can be determined unambiguously. For example, the neutron decay to ^{8}Be$_{g.s.}$ from the 2.78-MeV state was observed as a strong peak in the neutron time-of-flight (TOF) spectra by early works [5,6]. Therefore, we expected that we could determine I^π of the 2.78-MeV state from the β-decay asymmetry coincident with neutrons. Moreover, it is possible to eliminate neutron decays from higher excited states in ^{9}Be by gating the β-ray energy and selecting the dominant neutron decays. The spin-parity values of the excited states of ^{15,17}C were successfully assigned using a spin-polarized ^{15,17}B [28,31] beam produced by a projectile fragmentation method [32]. Using highly polarized ^{11}Li and ^{28}Na by an optical pumping method [33], the β-decay schemes of ^{11}Li [29] and ^{28}Na [30] were investigated, and the spin-parity values for ^{11}Be and ^{28}Mg were successfully assigned.

We report the experimental method and setup and the results for the unambiguous assignment of the spin-parity values of the states populated in ^{9}Li β decay. We demonstrate the validity of this method for the analysis of states with broad natural width.

II. EXPERIMENT

A. Principle of spin-parity assignment

In the present experiment, the β rays emitted from ^{9}Li were detected by β-ray telescopes, and the energies of the β-delayed neutrons were measured by the respective detectors for low- and high-energy neutrons. From the analysis of β-n coincidence events, the decay scheme of ^{9}Li was reconstructed. The most notable result was the use of spin-polarized ^{9}Li for the definite assignment of the spins and parities of the excited states in ^{9}Be.

The β rays emitted from a spin-polarized parent nucleus have an angular distribution $W(\theta)$. For the allowed transitions, $W(\theta)$ is expressed as a function of the emission angle θ from the polarization axis as

$$W(\theta) \propto 1 + (v/c)AP \cos\theta, \qquad (1)$$

where v, c, A, and P are the velocity of the emitted electron, light velocity, asymmetry parameter of the β transition, and polarization of the parent nucleus. In the case of a large Q_β, we can make the approximation $v/c \approx 1$. The asymmetry parameter A is related to the spins of both the initial (I_i) and the final states (I_f). For the allowed transition, the spin of the final state is restricted to either $I_f = I_i - 1$, I_i, or $I_i + 1$, and the parity is unchanged: $\pi_f = \pi_i$. For the three spin values allowed for the final state, the asymmetry parameter for β^- decay is expressed as follows:

$$A = \begin{cases} -1 & \text{for } I_f = I_i - 1, \\ \frac{-1/(I_i+1)-2\tau\sqrt{I_i/(I_i+1)}}{1+\tau^2} & \text{for } I_f = I_i, \\ \frac{I_i}{I_i+1} & \text{for } I_f = I_i + 1. \end{cases} \qquad (2)$$

Here τ is the mixing ratio of the Fermi to Gamow-Teller transitions, i.e., $\tau = C_V\langle 1 \rangle / C_A\langle \sigma \rangle$, where C_V and C_A are the Fermi and Gamow-Teller coupling constants, respectively, and $\langle 1 \rangle$ and $\langle \sigma \rangle$ are the corresponding nuclear matrix elements. The asymmetry parameter takes discrete values depending on the final-state spin I_f value. In the case of ^{9}Li$_{g.s.}$ ($I_i^\pi = 3/2^-$) β^- decay, the possible I_f^π values are $1/2^-$, $3/2^-$, and $5/2^-$, and the corresponding asymmetry parameter A is tabulated in Table II. In the second row of the table, a pure Gamow-Teller transition ($\tau \approx 0$) is assumed. This is a rather safe assumption for short-lived nuclei, where large differences in the single-

TABLE II. Possible final-state spin-parity values and associated asymmetry parameters of the allowed GT β^- transition from ^{9}Li$_{g.s.}$.

I_i^π (^{9}Li$_{g.s.}$)	I_f^π (^{9}Be)	A
	$1/2^-$	-1.0
$3/2^-$	$3/2^-$	-0.4
	$5/2^-$	$+0.6$

nucleon wave functions and in orbital energies are expected between protons and neutrons.

The largest difference in β-ray yield occurs between the two directions $\theta = 0$ (parallel to the polarization axis) and $\theta = \pi$ (antiparallel to the polarization axis), and is proportional to AP. The AP value is evaluated from the β-ray counting rates N_L and N_R in the β telescopes labeled Left (L) and Right (R) placed at $\theta = 0$ and $\theta = \pi$, respectively. The β-delayed neutrons are emitted by the strong interactions of nucleons of parity conservation. Therefore, they reveal the asymmetries of the β decays to states that emit radiation, so that we may determine the values of AP in Eq. (1) for the individual β-decay branches from the coincidences between β rays and β-delayed neutrons. The β-ray counts N_L and N_R obtained in coincidence with the β-delayed neutron associated with a specific state in $^9\mathrm{Be}^*$ are expressed as

$$N_L \propto \varepsilon_L^\beta \varepsilon_n (1 + AP),$$
$$N_R \propto \varepsilon_R^\beta \varepsilon_n (1 - AP),$$
(3)

where $\varepsilon_{L(R)}^\beta$ and ε_n are the detection efficiencies for β rays and β-delayed neutrons, respectively. Thus, the product of AP can be deduced from the ratio of Eqs. (3) as

$$AP = \frac{N_L \varepsilon_R^\beta - N_R \varepsilon_L^\beta}{N_L \varepsilon_R^\beta + N_R \varepsilon_L^\beta}.$$
(4)

The neutron detector efficiency ε_n is canceled out here. However, AP still includes ε_L^β and ε_R^β, which may cause further instrumental asymmetry. We therefore reverse the direction of the spin polarization by 180°. By using the β-ray counts, $N_L^\pm$ and $N_R^\pm$, for the two opposite spin polarizations ($\pm$), AP (which is free from the instrumental asymmetry) is obtained as

$$\rho = \frac{N_L^+/N_R^+}{N_L^-/N_R^-},$$
$$AP = \frac{\sqrt{\rho} - 1}{\sqrt{\rho} + 1}.$$
(5)

It is to be noted that the polarization P is common for all the β^- transitions feeding the different final states. As the result, if the initial-state spin I_i is known, we can evaluate P from the asymmetry of the β^- transition to a known state. The asymmetry parameter A for any transition to the other final states can then be determined. In addition to the level energies determined from the discrete energies of delayed neutrons, the spins and parities of the respective levels of $^9\mathrm{Be}^*$ can be determined unambiguously. The very discrete nature of the β-decay asymmetry parameter is also effective in unraveling information about hidden peaks in the energy spectrum of the delayed neutrons measured by the neutron detectors.

B. Experimental setup

The experiment was performed at ISAC, the radioactive nuclear beam facility of TRIUMF, where highly polarized alkali-metal ion beams are available by means of a collinear optical pumping technique [33]. The typical beam intensity
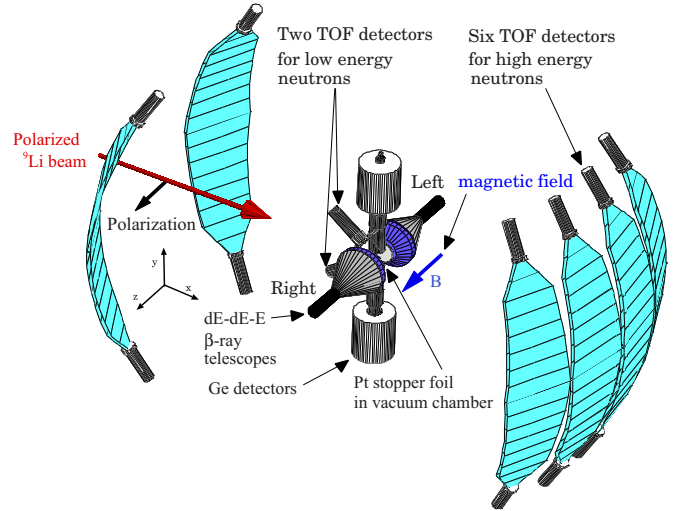

FIG. 1. (Color online) Experimental setup.

of a polarized $^9\mathrm{Li}$ beam with an energy of 30.5 keV is approximately 10^5 particles per second. Figure 1 shows a schematic view of the present setup. A polarized $^9\mathrm{Li}$ beam was incident onto a platinum stopper foil (10 μm thick), where an external static magnetic field ($\approx$22 mT) was applied to preserve the nuclear polarization. The direction of $^9\mathrm{Li}$ polarization was horizontal and perpendicular to the beam direction. The direction of $^9\mathrm{Li}$ polarization was reversed every 30 s by flipping the helicity of the pumping laser so as to cancel the instrumental asymmetry in the β-ray detectors. The radiations emitted in the decay of $^9\mathrm{Li}$ were detected by an assembly of detectors in the atmosphere. The β rays were detected by two ΔE-ΔE-E plastic scintillator telescopes. The telescopes were placed along the polarization axis (horizontal, $\theta = 0$, and $\theta = \pi$). The β-decay asymmetry AP was measured from the left-right asymmetry of the β counts ($N_L^\pm$ and $N_R^\pm$). The neutrons were detected over a wide energy range with two types of scintillation detectors. The neutron energies were determined by the TOF technique for β-neutron coincidence: High-energy neutrons ($E_n = 0.15$–9 MeV) were detected with six curved, large-area plastic scintillators (flight length, 1.48 m; thickness, 2 cm; arc length, 1.2 m; lateral width, 40 cm; $\varepsilon \Delta\Omega \approx 1.5 \times 10^{-2}$ for a 0.67-MeV neutron). The flight length of 148 cm was longer than the previously used values of 116 cm [5] and 28 cm [6] and therefore the resolving power was higher than in previous works [5,6]. For low-energy neutrons (3–600 keV), two $^6\mathrm{Li}$-doped glass scintillators were used (flight length, 13 cm; 50 mm $\phi \times$ 10 mm; $\varepsilon \Delta\Omega \approx 2 \times 10^{-3}$ for 250-keV neutrons). Two high-purity germanium (HPGe) detectors ($\varepsilon \Delta\Omega \approx 1.6 \times 10^{-2}$ for 1173-keV γ rays) were placed above and below the stopper. However, in the $^9\mathrm{Li}$ β-decay scheme, there have been no reports of β-delayed γ rays.

III. EXPERIMENTAL RESULTS AND DISCUSSION

A. Spin polarization of $^9\mathrm{Li}$

To deduce the β-decay asymmetry parameter A for each β transition from Eq. (5), the spin polarization P of $^9\mathrm{Li}$ has
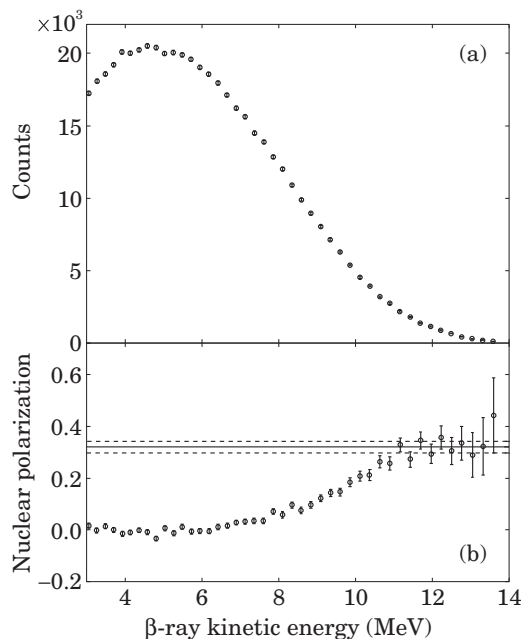
FIG. 2. (a) β-ray energy spectrum for all β transitions in ^{9}Li decay. (b) Measured spin polarization P as a function of β-ray energy. The high-energy trend is shown as a solid line, with the errors in the trend shown as dashed lines.

to be evaluated from the measured AP value and the known A value. In the case of ^{9}Be, the spin and parity values of the ground state are firmly assigned to be $3/2^-$ ($A = -0.4$) [24]. We evaluated the spin polarization P by setting a β-ray energy gate corresponding to the pure transition to the ground state. Figures 2(a) and 2(b) show the β-ray energy spectrum and the measured spin polarization P obtained from the ratio of the measured AP value to $A = -0.4$ for the ground state, as a function of β-ray energy, respectively. The measured P is almost 0 up to 8 MeV, gradually increases to about 0.3, and finally becomes constant at 0.3 around $Q_\beta = 13.6$ MeV. This indicates that contributions from states with $I = 5/2^-$ ($A = +0.6$) are mixed in the same strength as those from the states with negative A values ($A = -0.4$ and/or -1) and, therefore, the measured AP values became almost 0.

The β-ray end energy for the reported first negative-parity state of 2.43 MeV in ^{9}Be is 11.17 MeV. The first excited state of ^{9}Be is located at an excitation energy of $E_x = 1.684$ MeV, which corresponds to a β-ray end energy of 11.92 MeV. The first excited state has spin parity $1/2^+$, and, therefore, the β transition has not been reported owing to the first-forbidden transition. Using a β-ray energy gate for the range 12–13.6 MeV, it is possible to select the transition to the ground state of ^{9}Be. Indeed, the measured P value is constant in the range 11–13.6 MeV within the error. By setting the present gate, the spin-polarization of ^{9}Li was evaluated to be $P = +0.32 \pm 0.02$.

B. Analysis of neutron TOF spectrum and measured β-decay asymmetry parameter A as a function of neutron TOF

Figures 3(a) and 3(b) show the high-energy neutron TOF spectrum and the β-ray energy asymmetry parameter A as a
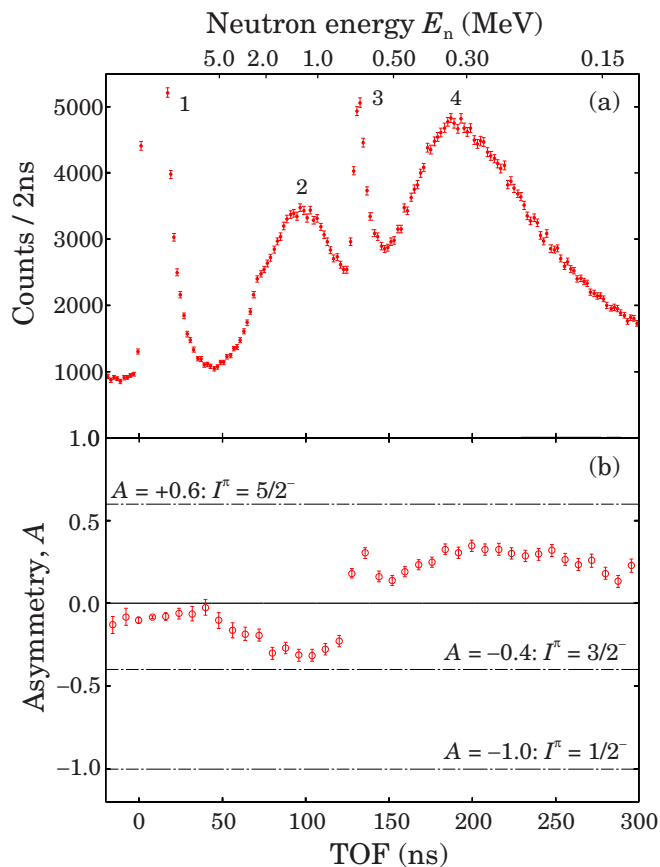

FIG. 3. (Color online) (a) High-energy neutron TOF spectrum and (b) β-decay asymmetry spectrum as functions of TOF with a β-ray energy gate of $E_\beta \geqslant 1.5$ MeV.

function of the neutron TOF, in the case of a β-ray energy gate of $E_\beta \geqslant 1.5$ MeV, respectively. The A values were obtained from the ratio of the measured AP value in coincidence with neutrons to the deduced spin-polarization $P = +0.32 \pm 0.02$. The expected β-asymmetry parameters -1.0 (for ^{9}Be* states with $I^\pi = 1/2^-$), -0.4 ($3/2^-$), and $+0.6$ ($5/2^-$) are shown by horizontal dot-dashed lines in Fig. 3(b).

In the TOF spectrum, we observed four prominent peaks, labeled 1–4. Peak 1, whose center position of 4.97 ns corresponds to the light velocity, is a prompt peak owing to Bremsstrahlung emitted from high-energy β rays, which were mainly scattered at the vacuum chamber. The structure of peak 1 follows the detector response function, which has a long tail around 50 ns. This is attributable to the low-energy threshold of the neutron counter to detect as low-energy a neutron as a few hundred keV. Peaks 2, 3, and 4 are similar to those observed in previous works [5,6]. In Refs. [5,6], peak 2 is identified as originating in the neutron transition from the 2.78-MeV [$\Gamma = 1.08(11)$ MeV] state [6] in ^{9}Be to the ^{8}Be ground state. Based on the narrow width of peak 3, the neutron channel for the peak was considered to be neutron channel (i) (see list of neutron channels in Sec. I) [5,6,10] from the 2.43-MeV state. In Refs. [5,6,10], peak 4 is considered to consist of the neutron transitions from the 2.43- and 2.78-MeV states to the first excited state of ^{8}Be. The energy spectrum of peak 4 was

precisely measured using ^{3}He neutron detectors by Nyman *et al.* [10]. The peak energy and full width at half maximum (FWHM) were about 0.25 and 0.30 MeV, respectively.

It is clearly seen that the asymmetry parameters drastically change at the prominent neutron peak positions and are consistent with or close to the expected values, indicating that these peaks are predominantly of a single peak and that small mixing of peaks originating from different I^π states smears out the asymmetry slightly.

Experimental results [9,10,14,16,17] for the energy measurement of ^{9}Li β-delayed α particles suggest that higher excited states such as the 5.59-, 7.94-, and 11.81-MeV states in ^{9}Be decay with neutron channels (i)–(iv). In the present neutron TOF measurement shown in Fig. 3, we can directly observe the neutron transitions (i)–(iv) from the higher excited states for the first time. To recognize new neutron transitions, deduce the properties of neutron decays, and evaluate the spin-parity values of the excited states in ^{9}Be from the neutron TOF spectrum and the asymmetry spectrum in Fig. 3, we performed fits for both spectra by considering all the possible neutron transitions from the ^{9}Be excited states listed in Table I except for the 11.283- and 11.81-MeV states. The 11.283- and 11.81-MeV states are excluded because the β-ray energies of $Q_\beta = 2.3$ and 1.8 MeV, respectively, for these states are too low to detect using the β-ray telescopes in the present experiment. Therefore, we considered the contributions from nine excited states in ^{9}Be. We present the details of the fitting procedure and the result of the analysis in the following sections.

1. Line shape of neutron TOF

For the fits in Fig. 3, we calculated the line shapes of neutron TOF considering the possible neutron-decay channels (i)–(iv):

$$F(t) = \sum_{k=1}^{10^6} \left[\int_0^\infty \delta(t - t'_k) \times \varepsilon(t'_k) \times \sigma(t, t'_k) dt'_k \right], \quad (6)$$

$$t'_k = \frac{\ell}{|\overrightarrow{v'_{nk}}|}, \quad (7)$$

$$\overrightarrow{v'_{nk}} = \begin{cases} \mathcal{L}(\overrightarrow{v_{nk}}, \overrightarrow{v_{^9\text{Be}k}}) & \text{(neutron decay from } ^9\text{Be)}, \\ \mathcal{L}(\overrightarrow{v_{nk}}, \overrightarrow{v'_{^5\text{He}k}}) & \text{(neutron decay from } ^5\text{He)}, \end{cases} \quad (8)$$

$$\overrightarrow{v'_{^5\text{He}k}} = \mathcal{L}(\overrightarrow{v_{^5\text{He}k}}, \overrightarrow{v_{^9\text{Be}k}}), \quad (9)$$

$$\overrightarrow{v_{xk}} = \sqrt{\frac{2E_{xk}}{m_x}} \frac{\overrightarrow{v_{xk}}}{|\overrightarrow{v_{xk}}|} \quad (x = n, \, ^9\text{Be}, \, ^5\text{He}). \quad (10)$$

The neutron TOF line-shape function $F(t)$ was numerically calculated by the Monte Carlo method and was expressed as a summation of 10^6 events. $F(t)$ consists of the δ function of the TOF t'_k, the neutron detection efficiency $\varepsilon(t'_k)$ as a function of TOF, and the detector response function $\sigma(t, t'_k)$ [28]. $\varepsilon(t'_k)$ and $\sigma(t, t'_k)$ were evaluated using the CECIL [34] code and from the prompt γ-ray peak 1, respectively. The TOF t'_k was calculated

from the flight length ℓ and the neutron velocity $\overrightarrow{v'_{nk}}$, which was affected by the Lorentz boost $\mathcal{L}$ caused by the recoil effects of ^{9}Be and ^{5}He, which were generated by ^{9}Li β decay and α decay of the ^{9}Be excited state. For example, $\mathcal{L}(\overrightarrow{v_{nk}}, \overrightarrow{v_{^9\text{Be}k}})$ means that the neutron velocity $\overrightarrow{v_{nk}}$ in the center-of-mass system of ^{9}Be was changed to $\overrightarrow{v'_{nk}}$ in the laboratory system by the Lorentz boost considering the ^{9}Be velocity $\overrightarrow{v_{^9\text{Be}k}}$. For $x = n$ (neutron), ^{9}Be, and ^{5}He particles, the velocity $\overrightarrow{v_{xk}}$ is defined as shown in Eq. (10) using the kinetic energy E_{xk} and mass m_x. Here isotropic two-body decay was assumed for determining the particle direction $\frac{\overrightarrow{v_{xk}}}{|\overrightarrow{v_{xk}}|}$.

When the initial and final states are broad, to calculate the kinetic energy E_{xk}, it is necessary to consider the natural widths expressed by the Lorentz function $L(E)$ for the decay energy $Q_x > 0$ in the center of mass of the two-particle system, which is expressed by the following equations:

$$Q_x = E_i - (E_f + \Delta m), \quad (x = n, \, ^9\text{Be}, \, ^5\text{He}) \quad (11)$$

$$L_i(E_i) = \frac{\Gamma_i/2\pi}{(E_i - E_{i0})^2 + (\Gamma_i/2)^2}, \quad (12)$$

$$L_f(E_f) = \frac{\Gamma_f/2\pi}{(E_f - E_{f0})^2 + (\Gamma_f/2)^2}. \quad (13)$$

The subscripts i and f indicate initial and final states for neutron, β, and α decays. $E_{i(f)}$, Δm, $\Gamma_{i(f)}$, and $E_{i0(f0)}$ are the excitation energy considering the natural width, the mass difference between initial and final states, the natural width, and the center value of the excitation energies. The kinetic energy E_{xk} was finally evaluated from the mass ratio between the decayed particles, for example, ^{8}Be* (^{5}He$_{\text{g.s.}}$) and a neutron.

The neutron TOF line shape was classified into three kinds of shapes according to the neutron-decay channel: channel (i)–(ii), channel (iii)–(iv), and peak 4, as shown in Fig. 3. Figure 4 shows three typical kinds of line shape for neutron decays to ^{8}Be$_{\text{g.s.}}$ [channel (i)], from ^{5}He$_{\text{g.s.}}$ [channel (iii)], and to ^{8}Be* (peak 4).
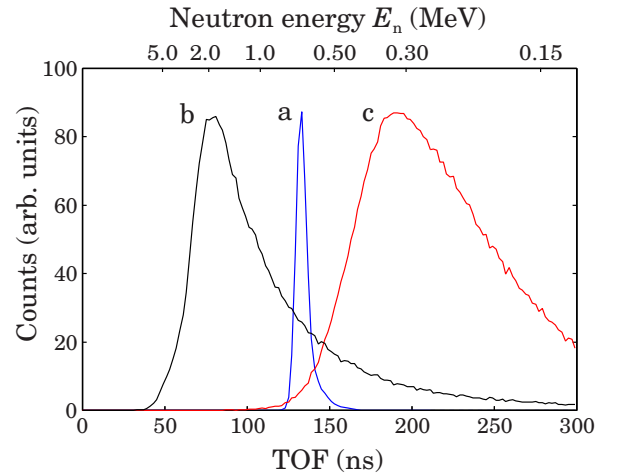

FIG. 4. (Color online) Calculated line shapes for (a) neutron decay channel (i), (b) neutron-decay channel (iii), and (c) peak 4.

For the neutron decay to ^{8}Be [channels (i) and (ii)], the line shape was mainly governed by the natural width of ^{9}Be and ^{8}Be. The effect of the Lorentz boost, originating from the recoil of ^{9}Be induced by β decay [10], must be taken into account only for channel (i) for the 2.43-MeV state. Because the natural width $\Gamma = 0.77$ keV of the 2.43-MeV state is narrow, the neutron emitted from the 2.43-MeV state to the ^{8}Be$_{\text{g.s.}}$ state was affected by the recoil effect ($\sigma \approx 30$ keV) [10]. For the other states of ^{9}Be, whose natural widths are more than a few hundred keV, the effect is negligible. The line shape (a) in Fig. 4, which corresponds to the neutron transition from the 2.43-MeV ($\Gamma = 0.77$ keV) state [24] in ^{9}Be to the ground state in ^{8}Be, followed the line shape for channel (i). The width and tail of the line shape were governed by the recoil effect of the β decay and the detector response, respectively.

In the case of neutron decay through ^{5}He [channels (iii) and (iv)], the line shape was mainly governed by the effect of the Lorentz boost originating from the recoil of ^{5}He induced by α decay. The energy of a neutron emitted from ^{5}He in the center-of-mass system is deduced to be 712 keV from the value $Q_n = 890$ keV [35]. The neutron energy is affected by the Lorentz boost, which causes the neutron energy to be widely spread. As a result, the TOF spectrum via ^{5}He$_{\text{g.s.}}$ has a broad width and an asymmetric shape owing to the conversion factor $|\partial E_n / \partial t|$ [28] for the conversion from an energy spectrum to a TOF spectrum. The line shape (b) in Fig. 4 for neutrons emitted from the 7.94-MeV ($\Gamma \approx 1$ MeV) state [24] in ^{9}Be to the ground state in ^{5}He follows that of channel (iii). The neutron energy was affected by the Lorentz boost, and the energy was therefore widely spread with a long tail and an asymmetric shape.

The line shape (c) in Fig. 4 corresponds to peak 4, as mentioned above. In the calculation, we employed a neutron energy spectrum with a peak energy of 0.25 MeV and FWHM of 0.30 MeV, as measured by Nyman *et al.* [10]. The peak position in the TOF spectrum was 190 ns, which corresponds to a neutron energy of 0.325 MeV. The peak shift from 0.25 MeV in the energy spectrum to 0.325 MeV in the TOF spectrum was caused by the conversion factor $|\partial E_n / \partial t|$. Thus, if we took the peak energy for a neutron peak with a broad width in the TOF spectrum, we would misread the exact peak energy. Therefore, it is essential to calculate broad line shapes to evaluate neutron transitions exactly.

Note that the effect of neutron scattering before entering the detector was not taken into account in the calculation. However, the validity of the calculated line shape was demonstrated in a previous ^{11}Li β-delayed neutron analysis [29].

2. Fitting procedure

In a least-χ^2 fit analysis for both neutron TOF and asymmetry parameter as a function of neutron TOF in Fig. 3, we assumed neutron transitions (i)–(iv) from all the excited states in ^{9}Be listed in Table I.

We fixed the level energy and width of the parent and daughter states, except for the 2.78-MeV state, to the listed values in Table I, and then calculated the line shapes $F_i(t)$, where the subscript i denotes a neutron transition. The 2.78-MeV state was excluded because unobserved neutron

transitions via ^{5}He$_{\text{g.s.}}$ were suggested in Refs. [14–17], and peak 2 in Fig. 3, which was considered to be a neutron transition from the 2.78-MeV state to ^{8}Be$_{\text{g.s.}}$, probably includes neutron transitions from ^{5}He$_{\text{g.s.}}$ and, therefore, the width of the 2.78-MeV state evaluated from the neutron TOF line shape would be narrower than the listed value of 1.08 MeV.

There are 36 line shapes $F_i(t)$, including the prompt peak 1 [$F_1(t)$]. Here we accounted for neutron transitions through channel (ii) from the 2.43- and 2.78-MeV states as being one neutron transition of peak 4 in Fig. 3, based on previous works [10]. The free parameters are the relative neutron-transition strength w_i (which is uncorrected by the efficiency of β-ray detectors), the discrete value of the β-decay asymmetry parameter A_i listed in Table II, the level energy and width of the 2.78-MeV state, the constant background w_{bg}, and the mixing ratio r of peak 4, which is necessary to calculate the asymmetry $A_4 = r A_{2.43 \text{ MeV}} + (1 - r) A_{2.78 \text{ MeV}}$ for the peak. Here $A_{2.43 \text{ MeV}}$ and $A_{2.78 \text{ MeV}}$ are the β-decay asymmetries for the 2.43- and 2.78-MeV states, respectively. By considering the efficiency of the β-ray detectors, which was evaluated by using GEANT3 [36], the neutron-transition strength I_{ni} (%) in ^{9}Li β-decay was evaluated from the deduced w_i. Note that the β-decay asymmetry parameter A_i is common for neutron transitions from the same state in ^{9}Be and that the asymmetry parameter for peak 1 (γ rays by Bremsstrahlung) and background (accidental coincidence events with the neutron counter) cause an intensity-weighted averaging of all of the β transitions. We therefore used the same asymmetry parameter for peak 1 and the background in the fitting.

We calculated all the line shapes corresponding to the mentioned neutron transitions. In the case of the 2.78-MeV state, the line shape was additionally calculated with $\Delta E_{i0} = 0.05$-MeV and $\Delta \Gamma_{i0} = 0.05$-MeV steps in the ranges $E_{i0} = 2.5$–2.8 MeV and $\Gamma = 0.15$–1.35 MeV, respectively.

The expected neutron TOF curve and the β-decay asymmetry curve as a function of the neutron TOF were calculated by an incoherent intensity-weighted summation $F_{\text{total}}(t)$ of the line shapes and an incoherent intensity-weighted averaging of the β-decay asymmetry $A_{\text{total}}(t)$ of the line shapes, respectively. Here χ^2 was calculated for all the possible combinations of asymmetry parameters. The number $N = 3^n$ of combinations depends on the number n of ^{9}Be excited states.

A least-χ^2 fit using MINUITE [37] was performed applying the equations

$$F_{\text{total}}(t) = \sum_{i=1}^{36} w_i F_i(t) + w_{\text{bg}},$$

$$A_{\text{total}}(t) = \frac{\sum_{i=1}^{36} A_i w_i F_i(t) + A_{\text{bg}} w_{\text{bg}}}{\sum_{i=1}^{36} w_i F_i(t) + w_{\text{bg}}},$$

$$\chi^2 = \frac{\sum_{i=1}^{160} [F_{\text{total}}(t) - D_{\text{TOF}}(t)]^2}{(\delta D_{\text{TOF}})^2} \qquad (14)$$

$$+ \frac{\sum_{i=1}^{40} [A_{\text{total}}(t) - D_{\text{A}}(t)]^2}{(\delta D_{\text{A}})^2},$$

where $D_{\text{TOF}}(t)$, $D_{\text{A}}(t)$, $\delta D_{\text{TOF}}(t)$, and $\delta D_{\text{A}}(t)$ are the experimental data of the neutron TOF and the β-decay asymmetry
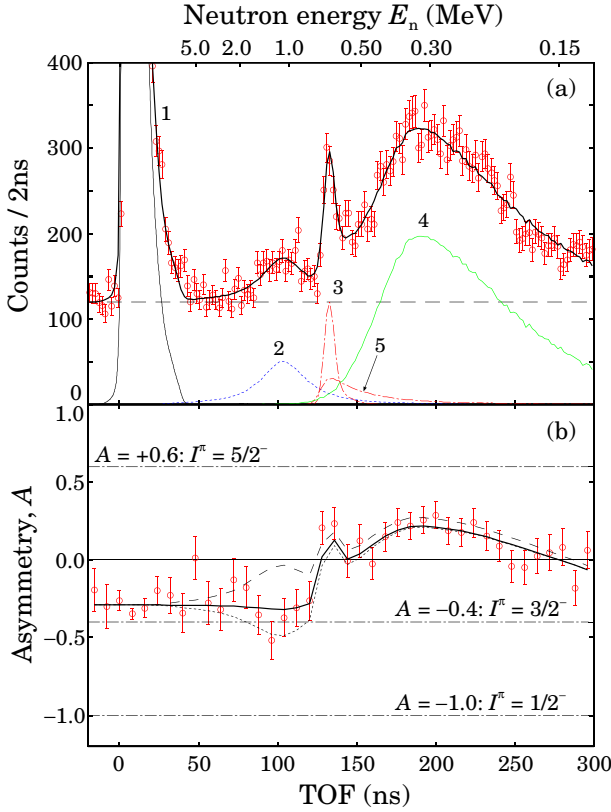
FIG. 5. (Color online) (a) High-energy neutron TOF spectrum and (b) β-decay asymmetry spectrum as functions of TOF gated at a β-ray energy of $E_\beta \geqslant 9.0$ MeV ($E_x \leqslant 4.6$ MeV). The thick black lines indicate the best fit obtained for the combination $I^\pi = 5/2^-$ and $3/2^-$ for the 2.43- and 2.78-MeV states, respectively. The dashed line in the TOF spectrum shows the background while the numbered peaks show the neutron-transition peaks in the spectrum. The dotted and dashed lines in the asymmetry spectrum are the calculated asymmetry lines for $I^\pi = 1/2^-$ and $5/2^-$ for the 2.78-MeV state.

and their associated errors. There were 160 and 40 data points in the neutron TOF and asymmetry spectra.

To eliminate the contributions from the higher excited states, the neutron TOF and associated asymmetry spectra gated at β-ray energies of $E_\beta \geqslant 9.0$ MeV (corresponding to an excitation energy of $E_x \leqslant 4.6$ MeV in ^{9}Be), $E_\beta \geqslant 6.5$ MeV ($E_x \leqslant 7.1$ MeV), and $E_\beta \geqslant 1.5$ MeV ($E_x \leqslant 12.1$ MeV) were analyzed. The transition strength I_{ni} and spin-parity value I^π for the neutron transitions from the 1.684-, 2.43-, 2.78-, and 3.049-MeV states for $E_\beta \geqslant 9.0$-, the 4.704-, and 5.59-MeV states for $E_\beta \geqslant 6.5$ MeV, and the 6.38-, 6.76-, and 7.94-MeV states for $E_\beta \geqslant 1.5$ MeV were mostly deduced from the analysis for the respective E_β gated spectra. Note that the same neutron line shapes were applied to the spectra for the different β-ray energy gates. The respective fitting results are described in the following sections.

3. Fitting for spectra gated at β-ray energy $E_\beta \geqslant 9$ MeV

Figures 5(a) and 5(b) show the neutron TOF and associated asymmetry spectra gated at a β-ray energy of $E_\beta \geqslant 9.0$ MeV ($E_x \leqslant 4.6$ MeV), respectively. The neutron transitions from the 2.43- and 2.78-MeV states were mainly selected in the spectra. Both spectra in Fig. 5 were fitted simultaneously using the calculated line shapes $F_{\text{total}}(t)$ and $A_{\text{total}}(t)$ in Eqs. (14). Note that all the possible neutron transitions from the ^{9}Be excited states listed in Table I were taken into account in the fitting. The fitting results confirm that only the neutron transitions from the 2.43- and 2.78-MeV states contributed to the neutron TOF in Fig. 5. The thick black solid lines in the TOF and the asymmetry spectra show the best fit of the total line shapes for the neutron peaks 1–5 listed in Table III and the constant background (dashed line) in Fig. 5(a). The blue (dotted line), red (dot-dashed line), and green (solid line for only peak 4) lines in Fig. 5 (a) indicate the negative ($I^\pi = 1/2^-$ or $3/2^-$) and positive ($5/2^-$) asymmetry values, and the mixing value between the negative and positive asymmetry values, respectively. The I_{ni} values (%) in ^{9}Li β decay, which were corrected by considering the efficiency of the β-ray detectors, are listed in Table III. In the present fitting, we neglect peaks with intensities I_{ni} less than 0.01%, which are insensitive to the present fitting.

TABLE III. β-delayed neutron transitions and their decay properties.

Neutron transition from ^{9}Be			$E_\beta \geqslant 9.0$		$E_\beta \geqslant 6.5$		$E_\beta \geqslant 1.5$		$E_\beta \geqslant 1.5$	
E_x (MeV)	peak	Transition	I^π	I_{ni} (%)	I^π	I_{ni} (%)	I^π	I_{ni} (%)	I^π	I_{ni} (%)
2.43	3	$^8\text{Be}_{\text{g.s.}} + n$	$5/2^-$	1.20(15)	$5/2^-$	1.25(13)	$5/2^-$	1.16(12)	$5/2^-$	1.16(12)
	4	$^8\text{Be}^* + n$	$5/2^-$		$5/2^-$		$5/2^-$	35.3(52)	$5/2^-$	35.3(52)
	5	$^5\text{He}_{\text{g.s.}} \to \alpha + n$	$5/2^-$	1.38(25)	$5/2^-$	1.12(17)	$5/2^-$	1.37(17)	$5/2^-$	1.30(16)
2.78	2	$^8\text{Be}_{\text{g.s.}} + n$	$3/2^-$	4.55(57)	$3/2^-$	2.59(36)	$3/2^-$	3.00(36)	$3/2^-$	2.68(39)
	4	$^8\text{Be}^* + n$	$3/2^-$		$3/2^-$		$3/2^-$	5.8(9)	$3/2^-$	5.8(9)
	9	$^5\text{He}_{\text{g.s.}} \to \alpha + n$					$3/2^-$	0.48(14)	$3/2^-$	0.56(19)
3.049		$^8\text{Be}_{\text{g.s.}} + n$				0.1(3)		0.09(8)		0.05(6)
4.704	6	$^5\text{He}_{\text{g.s.}} \to \alpha + n$			$1/2^-$	4.24(62)	$1/2^-$	2.29(35)	$3/2^-$	3.43(46)
5.59	7	$^5\text{He}_{\text{g.s.}} \to \alpha + n$			$5/2^-$	1.96(82)	$5/2^-$	1.39(26)		
	8	$^8\text{Be}^* + n$			$5/2^-$	1.17(93)	$5/2^-$	1.42(27)	$5/2^-$	1.54(26)
7.94	10	$^5\text{He}_{\text{g.s.}} \to \alpha + n$					$3/2^-$	6.79(76)	$3/2^-$	7.40(80)
Reduced χ^2				1.24		1.36		1.36		1.32

A minimum reduced χ^2 of 1.24 was obtained for the combination $I^\pi = 5/2^-$ and $3/2^-$ for the 2.43- and 2.78-MeV states, respectively. $I^\pi = 5/2^-$ for the 2.43-MeV state, which has been definitely assigned based on many experiment results [24], was confirmed. However, $I^\pi = 3/2^-$ for the 2.78-MeV state conflicts with the reported value of $1/2^-$ [14,24].

The TOF of the narrow peak 3 was 132.1 ± 1 ns, which corresponds to a neutron energy of $E_n = 665 \pm 10$ keV. The neutron channel for peak 3 was considered to be neutron channel (i) [5,6,10], based on the narrow width. The evaluated level energy for the neutron emitted state was 2.41(1) MeV, which is consistent with the 2.43-MeV ($\Gamma = 0.77$ keV) state [5,6,10]. (Hereafter, we produced the line shape $F(t)$ using $E_x = 2.41$ MeV.) Our observation of the neutron transition labeled 5 is the first to be reported. These neutrons were emitted from the 2.43-MeV state via ${}^5\text{He}_{\text{g.s.}}$, a transition that was suggested by Prezado and Borge *et al.* [14,15].

E_x of the state which emits neutrons corresponding to peak 2 was evaluated to be 2.83(5) MeV, consistent with the 2.78-MeV state. The natural width was evaluated to be $0.73^{+0.15}_{-0.09}$ MeV from the fitting, which is narrower than the reported value of 1.08(11) MeV [35]. We set $E_x = 2.83$ MeV and $\Gamma = 0.73^{+0.15}_{-0.09}$ MeV in the following fit. The expected narrow width suggests that there are neutron transitions around peak 2 in the neutron TOF spectrum which appear in the spectra with the wider β-ray energy gate.

The 2.78-MeV state also decays to the ground states in ${}^8\text{Be}$ (peak 2) and ${}^5\text{He}$ (peak 5). The contribution of peak 2 is essential in understanding both the neutron TOF and the asymmetry spectra.

An analysis of peak 4 is presented in Sec. III B 5 with the discussion of the fitting for the spectra gated at a β-ray energy gate of $E_\beta \geqslant 1.5$ MeV.

4. Fitting for spectra gated at β-ray energy $E_\beta \geqslant 6.5$ MeV

Figures 6(a) and 6(b) show the neutron TOF and associated asymmetry spectra gated at a β-ray energy of $E_\beta \geqslant 6.5$ MeV ($E_x \leqslant 7.1$ MeV), respectively. The neutron transitions in the spectra consist of transitions from the 2.43-, 2.78-, 4.704-, and 5.59-MeV states. The thick black solid lines in the TOF and the asymmetry spectra show the best fits of the total line shapes for the neutron peaks of 1–8 listed in Table III and the constant background. Again, all the possible neutron transitions from the ${}^9\text{Be}$ excited states listed in Table I were taken into account in the fitting, and it was confirmed that the neutron transitions from the 2.43-, 2.78-, 4.704-, and 5.59-MeV states contributed to the neutron TOF in Fig. 6.

A minimum reduced $\chi^2 = 1.36$ was obtained for the combination of $I^\pi = 5/2^-$, $3/2^-$, $1/2^-$, and $5/2^-$ for the 2.43-, 2.78-, 4.704-, and 5.59-MeV states, respectively. I^π assignments for the 2.43- and 2.78-MeV states were consistent with the results of $E_\beta \geqslant 9.0$ MeV. The β-delayed neutron transitions via ${}^5\text{He}_{\text{g.s.}}$ from the 4.704-MeV [$\Gamma = 743(55)$ keV] and 5.59-MeV [$\Gamma = 1.33(36)$ MeV] states were observed, and the transitions are consistent with the transition from the 5.0(5)-MeV [$\Gamma = 2.0(5)$ MeV] state suggested by Prezado and Borge *et al.* [14,15], which would identify the neutron
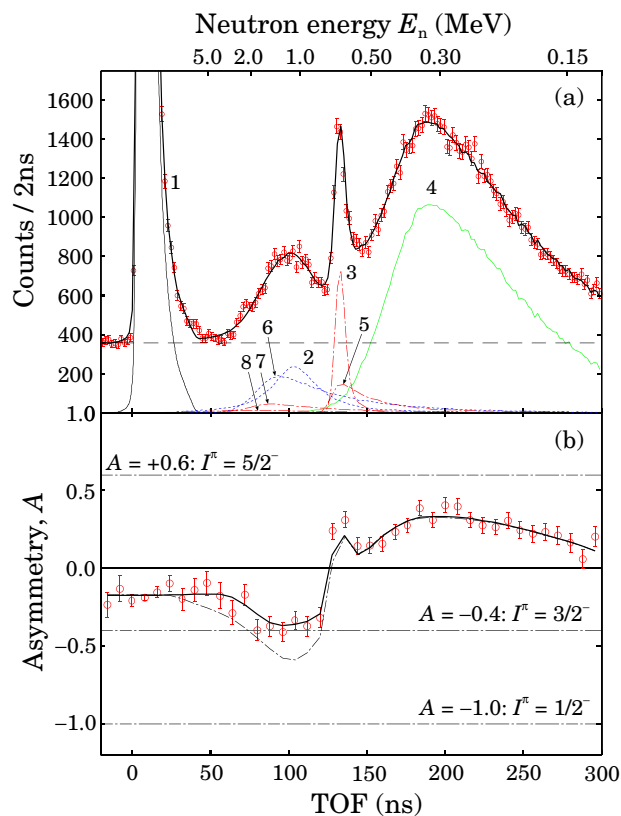

FIG. 6. (Color online) (a) High-energy neutron TOF spectrum and (b) β-decay asymmetry spectrum as functions of TOF gated at a β-ray energy of $E_\beta \geqslant 6.5$ MeV ($E_x \leqslant 7.1$ MeV). The thick black lines indicate the best fit obtained for the combination $I^\pi = 5/2^-$, $3/2^-$, $1/2^-$, and $5/2^-$ for the 2.43-, 2.78-, 4.704-, and 5.59-MeV states, respectively. The dashed line in the TOF spectrum shows the background, while the numbered peaks show the neutron-transition peaks in the spectrum. The dot-dashed line is the calculated asymmetry line for the combination $I^\pi = 1/2^-$ and $3/2^-$ for the 2.78- and 5.59-MeV states, which were reported in Ref. [14,24], indicating the fifth minimum value of the reduced $\chi^2 = 1.83$.

transitions from the 4.704- and 5.59-MeV states with that from the 5.0-MeV state. $I^\pi = 1/2^-$ and $5/2^-$ for the 4.704- and 5.59-MeV states, respectively, are suggested in the experiment. However, these I^π assignments are inconsistent with $I^\pi = (3/2)^+$ for the 4.704-MeV state reported in Ref. [24] and $I^\pi = 3/2^-$ for the 5.59-MeV state suggested in Refs. [12,14,15]. The dot-dashed line in Fig. 6(b) was calculated by considering a combination of the neutron transitions from the 2.78-MeV ($I^\pi = 1/2^-$) and 5.59-MeV ($3/2^-$) states according to the reported values in Ref. [14,24] (without the contribution of the 4.704-MeV state). The line systematically deviates from the data in the TOF region of 80–120 ns, and the evaluated reduced χ^2 was 1.83. This result also supports the present assignments of $I^\pi = 3/2^-$, $1/2^-$, and $5/2^-$ for the 2.78-, 4.704-, and 5.59-MeV states, respectively.

In the present measurement, a neutron transition with intensity $I_{ni} > 0.01$ was observed as being from the 3.049-MeV state. However, the intensity of 0.1(3)% was small and insensitive to the spectra. The small intensity indicates that the

β transition to the 3.049-MeV state would be forbidden, as reported in Ref. [35].

5. Fitting for spectra gated at β-ray energy $E_\beta \geqslant$ 1.5 MeV

Figures 7(a) and 7(b) show the neutron TOF and associated asymmetry spectra gated at a β-ray energy of $E_\beta \geqslant 1.5$ MeV ($E_x \leqslant 12.1$ MeV), respectively. Neutron transitions from all the excited states listed in Table I would contribute to the spectra. The thick black solid lines in the TOF and the asymmetry spectra show the best fits of the total line shapes for the neutron peaks of 1–10 listed in Table III and the constant background. The neutron decays via ^{5}He (peaks 9 and 10) were observed in the neutron TOF spectrum for the first time. The first and second minimum reduced $\chi^2 = 1.32$ and 1.36 were obtained with the combinations $I^\pi = \{5/2^-, 3/2^-, 3/2^-, 5/2^-, 3/2^-\}$ and $I^\pi = \{5/2^-, 3/2^-, 1/2^-, 5/2^-, 3/2^-\}$ for the $E_x = \{2.43, 2.78, 4.704, 5.59, 7.94\}$-MeV states, respectively, as shown in Table III, the only difference being the I^π assignment
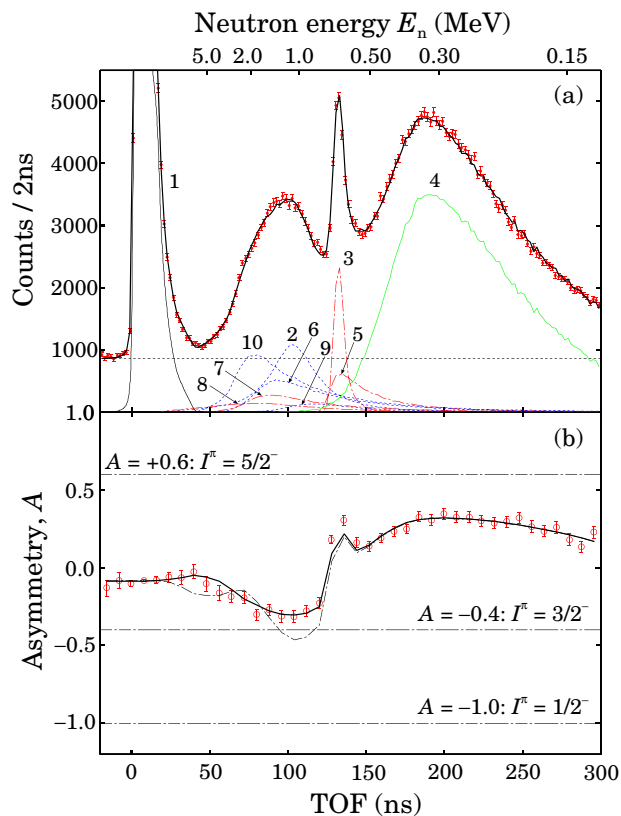
for the 4.704-MeV state. Considering the result for $E_\beta \geqslant 6.5$ MeV, we adopted the second minimum reduced χ^2 result, which proposes $I^\pi = 1/2^-$ for the 4.704-MeV state.

The neutron intensities I_{ni}'s for peaks 1–8 were in good agreement with each other, as shown in Table III. The I^π assignments for the 2.43- and 2.78-MeV states were consistent with the $E_\beta \geqslant 9.0$- and 6.5-MeV cases. As mentioned above, $I^\pi = 1/2^-$ and $5/2^-$ for the 4.704- and 5.59-MeV states were assigned, and, therefore, it was concluded that I^π of the 7.94-MeV state is $3/2^-$. This assignment is inconsistent with the previous report [9,14]. Again, the dot-dashed line in Fig. 7(b), calculated by considering the combination of neutron transitions from the 2.78-MeV ($I^\pi = 1/2^-$), 5.59-MeV ($3/2^-$), and 7.94-MeV ($5/2^-$) states reported in Refs. [14,24] (without the contribution of the 4.704-MeV state), systematically deviated from the data in the TOF region of 90–120 ns, and the evaluated reduced χ^2 was 2.24. This result also supports the present neutron transitions and I^π assignments. The neutron transition with intensity $I_{ni} = 0.09(8)$ was identified as being from the 3.049-MeV state and is consistent with that in Fig. 6. The intensity was small and insensitive to the spectra.

As a best estimate of I_{ni}, we adopted the I_{ni} values evaluated from the spectra gated at $E_\beta \geqslant 1.5$ MeV because of the higher statistics. The respective neutron-transition intensities from the 2.43- and 2.78-MeV states to ^{8}Be* can be deduced by using the evaluated intensity of peak 4 and the mixing ratio r evaluated from the fits to be $85.9 \pm 1.3\%$, which are consistent with $87.7 \pm 6.4\%$ ($E_\beta \geqslant 9$ MeV) and $89.5 \pm 2.1\%$ ($E_\beta \geqslant 6.5$ MeV) evaluated by considering the β-ray detection efficiency for the 2.43- and 2.78-MeV states. Here, there was large ambiguity in evaluating the intensity 32(16)% of peak 4 from the high-energy neutron TOF spectrum, because the peak distributed at the low-energy region was close to the detector threshold and we could not observe the whole line shape of the peak (more than 300 ns). Therefore, we deduced the neutron intensity of peak 4 from the low-energy neutron spectrum in Fig. 8. The ^{6}Li-doped glass scintillator is sensitive

FIG. 7. (Color online) (a) High-energy neutron TOF spectrum and (b) β-decay asymmetry spectrum as functions of TOF gated at a β-ray energy of $E_\beta \geqslant 1.5$ MeV ($E_x \leqslant 12.1$ MeV). The thick black lines indicate the best fit obtained for the combination $I^\pi = 5/2^-$, $3/2^-$, $1/2^-$, $5/2^-$, and $3/2^-$ for the 2.43-, 2.78-, 4.704-, 5.59-, and 7.94-MeV states, respectively. The dashed line in the TOF spectrum shows the background, while the numbered peaks show the neutron-transition peaks in the spectrum. The dot-dashed line is the calculated asymmetry line for the combination $I^\pi = 1/2^-$, $3/2^-$, and $5/2^-$ for the 2.78-, 5.59-, and 7.94-MeV states, which were reported in Ref. [14,24], indicating the seventh minimum value of the reduced $\chi^2 = 2.24$.
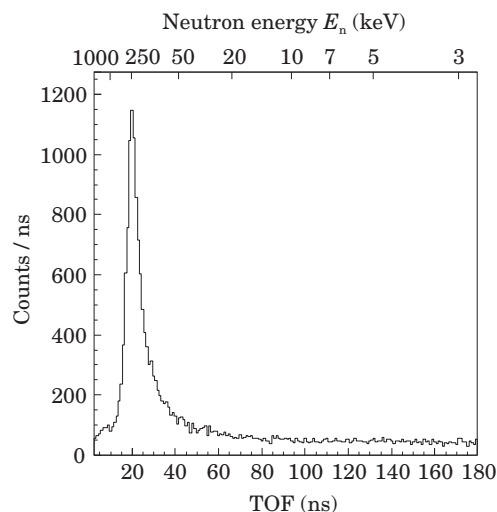

FIG. 8. TOF spectrum of low-energy neutrons measured by the ^{6}Li-doped glass scintillators.

to low-energy neutrons ($E_n < 1$ MeV) and has a resonance capture peak at a neutron energy of 245 keV.

One prominent peak around 250 keV, which corresponds to peak 4 in the high-energy neutron TOF spectrum, was observed. The peak structure is governed mainly by the resonance neutron-capture cross section of the ^{6}Li nucleus. From an integration between 3 and 600 keV, the neutron intensity of peak 4 was deduced to be $41.1 \pm 6\%$. The error is attributable to the ambiguity in the neutron-detection efficiency. The systematic error for integration in the energy region from 0 to 3 keV is negligible. There is no peak in the energy region from 3 to 250 keV. As mentioned above, peak 4 consists of low-energy neutron transitions from the 2.43- and 2.78-MeV states to ^{8}Be* [channel (ii)] [5,6,10]. Note that the β asymmetry of $+0.37 \pm 0.08$ measured by the glass scintillator was consistent with $+0.459 \pm 0.013$ evaluated from $r = 85.9 \pm 1.3\%$, $A_{2.43\,\text{MeV}} = +0.6$, and $A_{2.78\,\text{MeV}} = -0.4$ obtained from the high-energy spectra. Considering the mixing ratio r and neutron intensity obtained from the glass scintillator, the I_n values from the 2.43- and 2.78-MeV states to the ^{8}Be excited state were evaluated to be $35.3 \pm 5.2\%$ and $5.8 \pm 0.9\%$, respectively.

C. Decay scheme and levels in ^{9}Be

Figure 9 shows the β-decay scheme of ^{9}Li determined from the present experimental results. The β-decay intensity I_β and the log ft value were compared with the latest compilation [24] and the previous works [10,14] listed in Table IV. Here, we propose a level energy E_x of 2.41(1) MeV and 2.83(5) MeV ($\Gamma = 0.73^{+0.15}_{-0.09}$ MeV) for the 2.43- and 2.78-MeV states reported in the compilation [24], respectively. The log ft values in the range from 4.39 to 5.78 confirmed the analysis based on the β-decay asymmetry of the allowed transitions. In the following sections, we discuss the excited levels that emit neutrons observed in the present work.

1. Ground state with $I^\pi = 3/2^-$

The ground state of ^{9}Be was reported to be populated by β decay with a large branching ratio of 49.2% [24], and the spin-parity value of $I^\pi = 3/2^-$ has been firmly assigned by several experiments [24]. For example, from a coupled-channels analysis for the angular distributions of the ^{9}Be$(\alpha,\alpha')^9$Be reaction experiment [8], the I^π values of the 0-, 2.43-, and 6.38-MeV states were assigned to be $3/2^-$, $5/2^-$, and $7/2^-$, respectively. They were considered to be members of the $K^\pi = 3/2^-$ rotation band. In the present measurement, the summation of neutron intensities was 59.1(54)%, and no β-delayed γ rays were observed. As a result, a β-decay strength of 40.9(54)% to the ground state of ^{9}Be was evaluated, comparable to the reported value of 49.2(9)%.

2. 2.43-MeV state with $I^\pi = 5/2^-$

The properties, such as the energy and spin-parity value, of the 2.43-MeV state ($I^\pi = 5/2^-$) with a narrow width of $\Gamma = 0.77$ keV have been confirmed by several experiments (references in Ref. [24]). Neutron transitions from the 2.43-MeV state to ^{8}Be$_{\text{g.s.}}$ [channel (i)] and ^{8}Be^{2+} states [channel

(ii)] were measured and confirmed by Macefield *et al.* [5], Chen *et al.* [6], and Nyman *et al.* [10]. The measured neutron transitions from the 2.43-MeV state and the I^π assignment were consistent with the previous results [5,6,10,14]. The good agreement of I^π indicates the reliability of the present methodology.

3. 2.78-MeV state with $I^\pi = 3/2^-$

The 2.78 ± 0.12-MeV ($I^\pi = 1/2^-$, $\Gamma = 1.08(11)$ MeV) state [24] was first found to be 3.0 ± 0.1 MeV from β-delayed neutron measurements (TOF method) with decay channel (i) (^{8}Be $+ n$) by Macefield *et al.* [5] and was confirmed to be 2.78 ± 0.12 MeV from β-delayed neutron measurements by Chen *et al.* [6]. Owing to the higher resolving power of the neutron TOF detector than those used in previous work and the β-ray energy gate, E_x and Γ were determined to be 2.83(5) and $0.73^{+0.15}_{-0.09}$ MeV, respectively. The strengths of neutron transitions through channels (i) and (ii) were consistent with previous work [9,10], which evaluated the strength from β-delayed charged-particle measurements. The β-decay strength and log ft value in the present work are consistent with those of previous work [9,10,14]. However, the present proposed $I^\pi = 3/2^-$ for the state is inconsistent.

Prezado and Borge *et al.* [14,15] assigned $I^\pi = 1/2^-$ by considering only the angular correlation of decay channel (iii) (decay to ^{5}He$_{\text{g.s.}}$). However, the gated region for the analysis of the angular correlation seemed to include decay channels (ii) (decay to ^{8}Be*) and (iii). The contribution from decay channel (ii) gives two possible angular correlation of an isotropic one and the same one as channel (iii). In the analysis, they did not show any calculated fitting line in which all the possible correlations were taken into account. They could not measure the neutron decay of the 2.78-MeV state through ^{8}Be$_{\text{g.s.}}$ because the energies of the α particles were lower than the thresholds of the detectors. Therefore, they could not show the consistency of the assignment from the neutron decay through ^{8}Be$_{\text{g.s.}}$.

4. 3.049-MeV state with $I^\pi = 5/2^+$

I^π of the 3.049-MeV state has been proposed to be $5/2^+$ based on the detection of d-wave neutrons associated with ^{8}Be$_{\text{g.s.}}$ in photo-neutron angular-distribution measurements [1]. The d-wave neutrons emitted from the reaction ^{7}Li$(^3$He$,p)^9$Be [3] also support the I^π assignment, assuming a decay to ^{8}Be$_{\text{g.s.}}(0^+)$ as β decay to the state is forbidden owing to parity change. The present measured β-decay strength of 0.09(8) corresponding to log $ft = 7.55(40)$ indicates that the β transition is forbidden. Owing to the weak and forbidden transition, it was difficult to assign the spin-parity directly. Therefore, we adopted $I^\pi = 5/2^+$ from the previous work [1,3,24].

5. 4.704-MeV state with $I^\pi = 1/2^-$

I^π of the 4.704-MeV state was proposed to be $(3/2$ or $5/2)^+$ by assuming an s-wave neutron associated with ^{8}Be*(2^+) in photo-neutron angular-distribution measurements [1]. In an (e,e') experiment [4], $I^\pi = (3/2)^+$ for the 4.704-MeV state was proposed and referred to in the latest compilation [24].
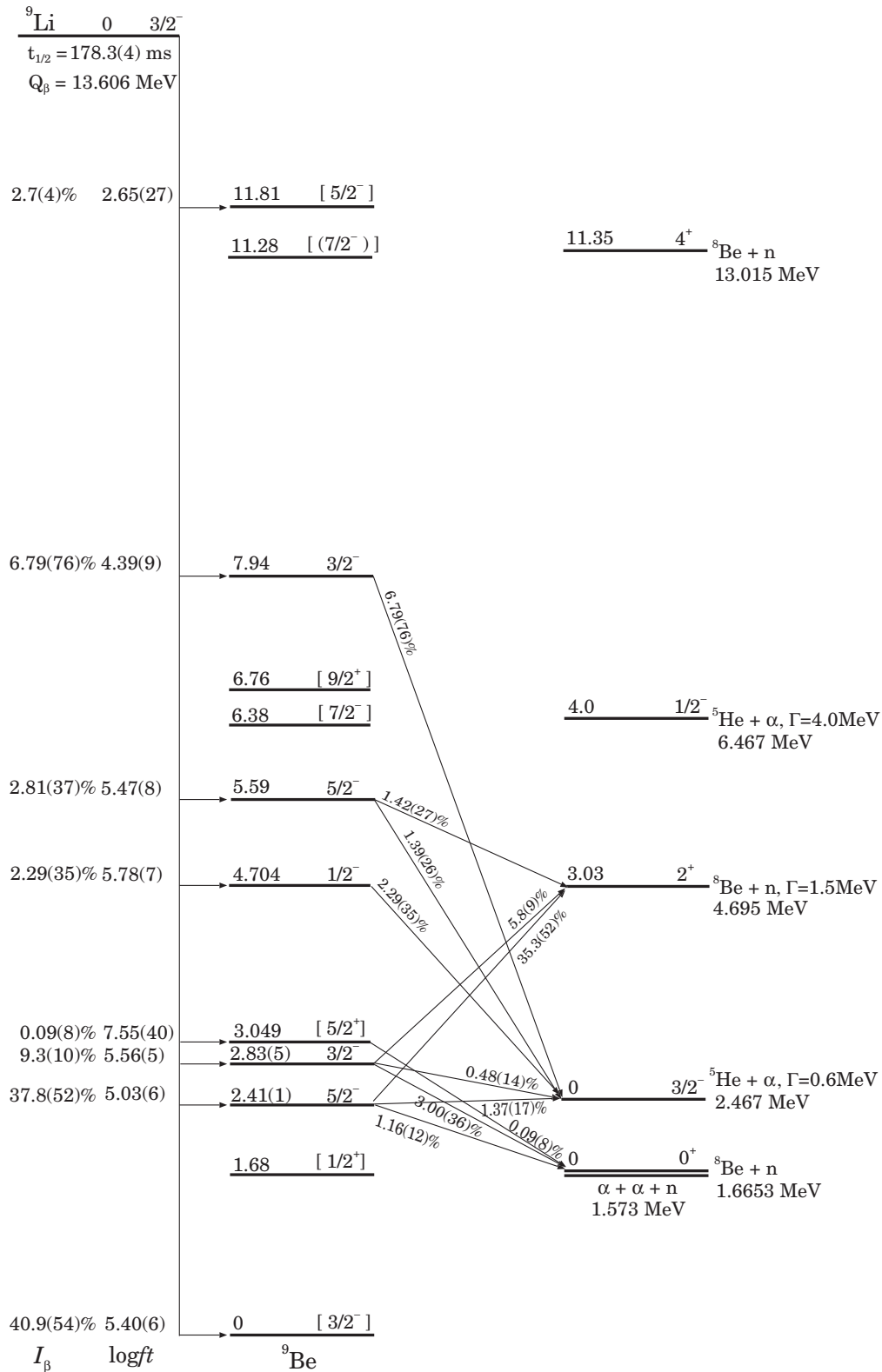
FIG. 9. Level and decay schemes of ^{9}Be established in the present work. The level energy and I^π in square brackets for the ^{9}Be states are from Ref. [24].

However, for the neutron decay of the 4.704-MeV state, there have been two conflicting reports of s-wave neutrons [1] associated with ^{8}Be(2^+) and d-wave neutrons [7] associated with ^{8}Be(0^+). The energy resolution in the work reported in Ref. [7] was poor and they did not take into account the contribution of the neutron decay to the ^{5}He($3/2^-$) state in their I^π assignments. Therefore, there is ambiguity in the spin-parity assignment for the 4.704-MeV state. In the

TABLE IV. Experimental energy levels in ^{9}Be and their decay properties.

^{9}Be		Present work			Compilation [24]		Ref. [10]		Ref. [14]	
E_x (MeV)	Γ (keV)	I^π	I_β (%)	$\log(ft)$	I^π	I_β (%)	I^π	I_β (%)	I^π	I_β (%)
0.00	Stable[a]	$3/2^{-}$[a]	40.9(54)	5.40(6)	$3/2^-$	49.2(9)	$3/2^-$	50(3)	$3/2^-$	49.2(9)[a]
2.41(1)	0.77[a]	$5/2^-$	37.8(52)	5.03(6)	$5/2^-$	29.7(30)	$5/2^-$	30(3)	$5/2^-$	31.9(34)
2.83(5)	$0.73^{+0.15}_{-0.09}$ MeV	$3/2^-$	9.3(10)	5.56(5)	$1/2^-$	15.8(3)	$1/2^-$	16(3)	$1/2^-$	11.6(22)
3.049[a]	282[a]	$5/2^{+}$[a]	0.09(8)	7.55(40)	$5/2^+$					
4.704[a]	743[a]	$1/2^-$	2.29(35)	5.78(7)	$(3/2)^+$					
5.59[a]	1330[a]	$5/2^-$	2.81(37)	5.47(8)	$(3/2)^-$				$3/2^-$	3.15(40)
7.94[a]	1000[a]	$3/2^-$	6.79(76)	4.39(9)	$(5/2^-)$	1.5(5)	$(1/2^-)$[b]	$\leqslant$2	$5/2^-$	1.5(4)
11.81[a]	400[a]	$5/2^{-}$[a]	2.7(4)[c]	2.65(27)	$5/2^-$	2.7(2)		2.7(2)	$5/2^-$	2.7(4)

[a]From the latest compilation [24].
[b]From Ref. [9].
[c]From Ref. [14].

present experiment, we observed the β-decay transition to the state with $\log ft = 5.78(7)$, which indicates an allowed β transition and a negative-parity state, and, therefore, we assign $I^\pi = 1/2^-$. The neutron transition from the state is one of the components of the neutron transition from the 5.0(5)-MeV [$\Gamma = 2.0(5)$ MeV] state which Prezado *et al.* [14] proposed as a new state.

6. 5.59-MeV state with $I^\pi = 5/2^-$

Dixit *et al.* discovered the 5.59(10)-MeV [$\Gamma = 1.33(36)$] state and tentatively assigned $I^\pi = (3/2^-)$ based on proton-scattering experiments [12]. In the present experiment, we observed neutrons from the 5.59-MeV state, which would be another component of the neutron transition from the 5.0-MeV state with $I^\pi = 3/2^-$ [14], found by Prezado *et al.* We identified the neutron transition from the 5.0-MeV state as being from the 4.704- and 5.59-MeV states, and assigned $I^\pi = 5/2^-$ for the 5.59-MeV state, based on the neutron TOF and β-decay asymmetry spectra with β-ray energy gates.

7. 7.94-MeV state with $I^\pi = 3/2^-$

I^π of the 7.94-MeV state was reported to be $(1/2)^-$ in the earlier compilation [26], but $(5/2)^-$ in the recent compilation [24], based on an unpublished thesis [27]. Prezado *et al.* proposed $I^\pi = 5/2^-$ from the α-α angular correlation [14], but I^π has not been assigned definitely. We propose $I^\pi = 3/2^-$ in the present work, determined from the combination assignments of the 4.704- and 5.59-MeV states by a careful analysis of the spectra.

D. Comparison with theoretical calculations

We compared the experimental results with the theoretical predictions by two kinds of shell-model calculations [19,38], antisymmetrized molecular dynamics (AMD) [21] and microscopic cluster model (MRM) [23], as shown in Fig. 10. We conducted the shell-model calculations with the CKIPN [19] and PWTPN [38] interactions using the NUSHELLX code [39]. The model space was restricted to the p shell, such as the $\pi(p1/2)$, $\pi(p3/2)$, $\nu(p1/2)$, and $\nu(p3/2)$ orbits. To estimate the strength of β transitions, the wave function of the parent

nucleus ^{9}Li$_{\text{g.s.}}$ was also deduced. The validity of these wave functions was examined by calculating the magnetic moment of ^{9}Li$_{\text{g.s.}}$. The experimental value of the ^{9}Li$_{\text{g.s.}}$ magnetic moment $\mu = 3.4391(6)\mu_n$ [35] was reasonably reproduced to be $\mu_{\text{calc}} = 3.376$ [19] and 3.312 [38], respectively. In Fig. 10, we show the calculated negative-parity states with level energy E_x, spin parity I^π, β-decay branching ratio I_β, and $\log ft$ value. These states were populated by allowed β-transitions of ^{9}Li. The present experimental results including E_x, I_β, $\log ft$ value, and I^π enabled us to perform a comparison on a level-by-level basis.

The thin solid and dashed lines in Fig. 10 denote the correspondences and the possible candidates, respectively, between the experimental and theoretical levels. The shell-model calculations by CKIPN [19] and PWTPN [38] interactions below $E_x = 8$ MeV in terms of E_x, I_β, $\log ft$ value, and I^π are in good agreement with the experimental data, except for the I^π assignment for the 2.83- and 4.704-MeV states. A candidate for the first $1/2^-$ state is as high as $E_x = 4.704$ MeV. From a simple consideration of the wave function of the $1/2^-$ state, the wave function $[(\nu p1/2)(\nu p3/2)^2]^{1/2^-} \otimes [(\pi p3/2)^2]^{0^+}$ is dominant (45% in the case of PWTPN interaction), and a $1/2^-$ state should be located close to the first $3/2^-$ state and below the second $3/2^-$ state. Indeed, the location of the $1/2^-$ state calculated by CKIPN [19] and PWTPN [38] interactions is around 3 MeV. However, the 2.83- and 4.704-MeV states with $I^\pi = 3/2^-$ and $I^\pi = 1/2^-$ would correspond with the states around 5 and 3 MeV, with $I^\pi = 3/2^-$ and $I^\pi = 1/2^-$, respectively, as predicted by theoretical calculations, and the first $1/2^-$ state and second $3/2^-$ state are inverted in the present experiment. In this case, considering the I_β and $\log ft$ values of the 2.83-, 5.59-, and 7.94-MeV states, the PWTPN effective interaction reproduced the experimental data better than the CKIPN effective interaction. Between $E_x = 9$ and 13 MeV, several states are predicted by the shell-model calculations. Both shell-model calculations suggested that the second $1/2^-$ state is around 9–13 MeV with a β transition probability up to $I_\beta \approx 1.3\%$. However, we could not recognize a state with an intense I_β in the present experiment. Although the shell-model calculations with p-shell configurations were in overall good agreement with the present results, this might
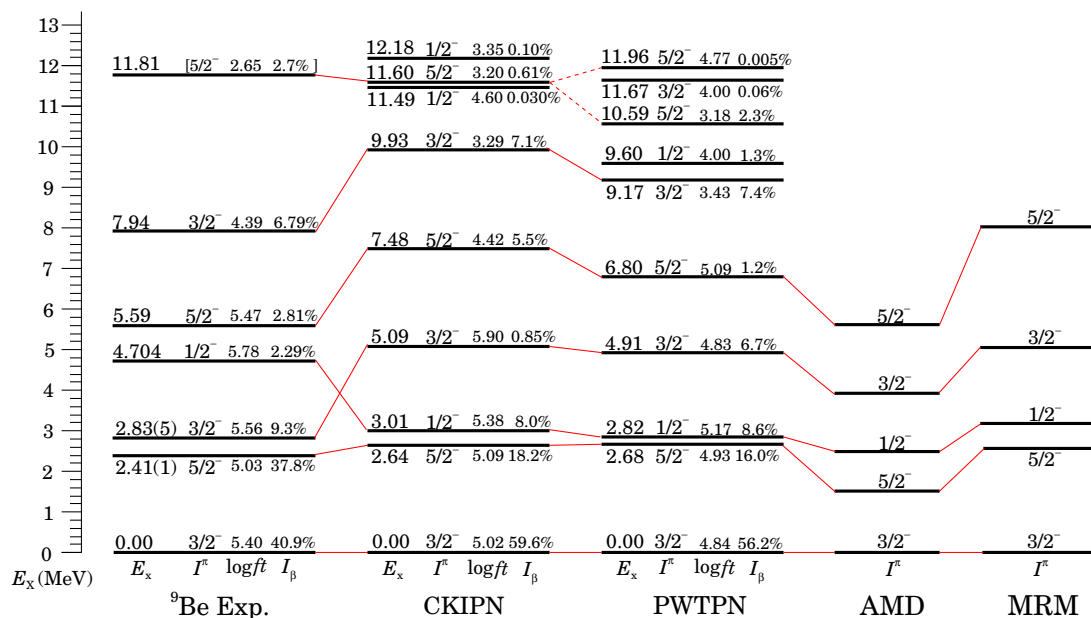
FIG. 10. (Color online) Comparison between experimental results and theoretical calculations.

indicate a limitation of the present effective interactions used for application to unbound states.

An AMD calculation [21] systematically predicted a lower E_x than the experimental results, and E_x and I^π were well predicted by MRM calculations [23]. The theoretical works on the shell-model [19,20,38], AMD [21], and MRM [22,23] predicted that the low-lying energy levels are located in the sequence $I^\pi = 3/2^-, 5/2^-, 1/2^-$, and $3/2^-$. However, in the present work, the order is $I^\pi = 3/2^-, 5/2^-, 3/2^-$, and $1/2^-$. No theoretical prediction was consistent with the present I^π assignment for the 2.83- and 4.704-MeV states.

IV. SUMMARY

We have established the level scheme and the decay scheme of ^{9}Be from β-delayed neutron spectroscopy with spin-polarized ^{9}Li. The neutron decays via ^{5}He$_{g.s.}$ were newly measured in the neutron TOF spectrum and identified based on the β-asymmetry spectra in coincidence with the neutron TOF. Based on these results, the neutron-decay scheme of ^{9}Li has been dramatically improved. The present results in terms of the β-decay branching ratio I_β and log ft value were consistent with those of the previous works [10,14,15]. However, the I^π assignments were inconsistent with those of the previous

works [10,14,15]. A firm spin-parity assignment was made for the known level of 2.43 MeV ($I^\pi = 5/2^-$) in ^{9}Be. From the analysis of the asymmetry spectra for the neutron transition, we confidently suggested a I^π value of $3/2^-$ for the 2.78-MeV state. For the 4.704-, 5.59-, and 7.94-MeV states, we proposed spin-parity values of $I^\pi = 1/2^-, 5/2^-$, and $3/2^-$ from the β-ray energy gated spectra. A further experiment measuring β-delayed neutrons and α particles with low threshold would be necessary to verify the accuracy of the present assignment for I^π.

A detailed comparison with the shell-model calculations with a level-by-level basis was performed. We found an overall good reproduction of the shell-model calculations with p-shell configurations.

[1] M. J. Jakobson, Phys. Rev. **123**, 229 (1961).

[2] R. R. Spencer, G. C. Phillips, and T. E. Young, Nucl. Phys. **21**, 310 (1961).

[3] P. R. Cheristensen and C. L. Cocke, Nucl. Phys. **89**, 656 (1966).

[4] H. G. Clerc, K. J. Wetzel, and E. Spamer, Nucl. Phys. A **120**, 441 (1968).

[5] B. E. F. Macefield, B. Wakefield, and D. H. Wilkinson, Nucl. Phys. A **131**, 250 (1969).

[6] Y. S. Chen, T. A. Tombrello, and R. W. Kavanagh, Nucl. Phys. A **146**, 136 (1970).

[7] B. Rendic, N. D. Gabitzsch, V. Valkovic, and W. V. Witsch, Nucl. Phys. A **178**, 49 (1971).

[8] M. N. Harakeh, J. V. Popta, A. Saha, and R. H. Siemssen, Nucl. Phys. A **344**, 15 (1980).

[9] M. Langevin, C. Dàtraz, D. Guillemaud, F. Naulin, M. Epherre, R. Klapisch, S. K. T. Mark, M. De Saint Simon, C. Thibault, and F. Touchard, Nucl. Phys. A **366**, 449 (1981).

[10] G. Nyman, R. Azuma, P. Hansen, B. Jonson, P. O. Larsson, S. Mattsson, A. Richter, K. Riisager, O. Tengland, K. Wilhelmsen, and T. I. Collaboration, Nucl. Phys. A **510**, 189 (1990).

[11] J. P. Glickman, W. Bertozzi, T. N. Buti, S. Dixit, F. W. Hersman, C. E. Hyde-Wright, M. V. Hynes, R. W. Lourie, B. E. Norum, J. J. Kelly, B. L. Berman, and D. J. Millener, Phys. Rev. C **43**, 1740 (1991).

[12] S. Dixit, W. Bertozzi, T. N. Buti, J. M. Finn, F. W. Hersman, C. E. Hyde-Wright, M. V. Hynes, M. A. Kovash, B. E. Norum, J. J. Kelly, A. D. Bacher, G. T. Emery, C. C. Foster, W. P. Jones, D. W. Miller, B. L. Berman, and D. J. Millener, Phys. Rev. C **43**, 1758 (1991).

[13] Y. Prezado, U. Bergmann, M. J. G. Borge, J. Cederkäll, C. A. Diget, L. M. Fraile, H. O. U. Fynbo, H. Jeppesen, B. Jonseon, M. Meister, T. Nilsson, G. Nyman, K. Riisager, O. Tengblad, L. Weissman, and K. W. Rolander, Phys. Lett. B **576**, 55 (2003).

[14] Y. Prezado, M. J. G. Borge, C. A. Diget, L. M. Fraile, B. R. Fulton, H. O. U. Fynbo, H. B. Jeppesen, B. Jonson, M. Meister, T. Nilsson, G. Nyman, K. Riisager, O. Tengblad, and K. Wilhelmsen, Phys. Lett. B **618**, 43 (2005).

[15] M. J. G. Borge, Y. Prezado, O. Tengblad, H. O. U. Fynbo, K. Riisager, and B. Jonson, Phys. Scr. **T125**, 103 (2006).

[16] P. Papka, T. A. D. Brown, B. R. Fulton, D. L. Watson, S. P. Fox, D. Groombridge, M. Freer, N. M. Clarke, N. I. Ashwood, N. Curtis, V. Ziman, P. McEwan, S. Ahmed, W. N. Catford, D. Mahboub, C. N. Timis, T. D. Baldwin, and D. C. Weisser, Phys. Rev. C **75**, 045803 (2007).

[17] T. A. D. Brown, P. Papka, B. R. Fulton, D. L. Watson, S. P. Fox, D. Groombridge, M. Freer, N. M. Clarke, N. I. Ashwood, N. Curtis, V. Ziman, P. McEwan, S. Ahmed, W. N. Catford, D. Mahboub, C. N. Timis, T. D. Baldwin, and D. C. Weisser, Phys. Rev. C **76**, 054605 (2007).

[18] S. Lukyanov, A. Denikin, E. Voskoboynik, S. Khlebnikov, M. Harakeh, V. Maslov, Y. Penionzhkevich, Y. Sobolev, W. Trzaska, G. Tyurin, and K. Kuterbekov, J. Phys. G **41**, 035102 (2014).

[19] S. Cohen and D. Kurath, Nucl. Phys. **73**, 1 (1965).

[20] F. C. Barker, Nucl. Phys. **83**, 418 (1966).

[21] Y. Kanada-En'yo, H. Horiuchi, and A. Ono, Phys. Rev. C **52**, 628 (1995).

[22] P. Descouvemont, Eur. Phys. J. A **12**, 413 (2001).

[23] K. Arai, P. Descouvemont, D. Baye, and W. N. Catford, Phys. Rev. C **68**, 014310 (2003).

[24] D. R. Tilley, J. H. Kelley, J. L. Godwin, D. J. Millener, J. E. Purcell, C. G. Sheu, and H. R. Weller, Nucl. Phys. A **745**, 155 (2004).

[25] J. P. Elliott, Technical Report NYO-2271, University of Rochester, 1958.

[26] F. Ajzenberg-selove, Nucl. Phys. A **490**, 1 (1988).

[27] L. J. de Bever, Ph.D. thesis, Utrecht university, 1993.

[28] H. Miyatake, H. Ueno, Y. Yamamoto, N. Aoi, K. Asahi, E. Ideguchi, M. Ishihara, H. Izumi, T. Kishida, T. Kubo, S. Mitsuoka, Y. Mizoi, M. Notani, H. Ogawa, A. Ozawa, M. Sasaki, T. Shimoda, T. Shirakura, N. Takahashi, S. Tanimoto, and K. Yoneda, Phys. Rev. C **67**, 014306 (2003).

[29] Y. Hirayama, T. Shimoda, H. Izumi, A. Hatakeyama, K. P. Jackson, C. D. P. Levy, H. Miyatake, M. Yagi, and H. Yano, Phys. Lett. B **611**, 239 (2005).

[30] K. Kura, K. Tajiri, T. Shimoda, A. Odahara, T. Hori, M. Kazato, T. Masue, M. Suga, A. Takashima, T. Suzuki, T. Fukuchi, Y. Hirayama, N. Imai, H. Miyatake, M. Pearson, C. D. P. Levy, and K. P. Jackson, Phys. Rev. C **85**, 034310 (2012).

[31] H. Ueno, H. Miyatake, Y. Yamamoto, S. Tanimoto, T. Shimoda, N. Aoi, K. Asahi, E. Ideguchi, M. Ishihara, H. Izumi, T. Kishida, T. Kubo, S. Mitsuoka, Y. Mizoi, M. Notani, H. Ogawa, A. Ozawa, M. Sasaki, T. Shirakura, N. Takahashi, and K. Yoneda, Phys. Rev. C **87**, 034316 (2013).

[32] K. Asahi, M. Ishihara, N. Inabe, T. Ichihara, T. Kubo, M. Adachi, H. Takahashi, M. Kouguchi, M. Fukuda, D. Mikolas, D. J. Morrissey, D. Beaumel, T. Shimoda, H. Miyatake, and N. Takahashi, Phys. Lett. B **251**, 488 (1990).

[33] C. Levy, A. Hatakeyama, Y. Hirayama, R. Kiefl, R. Baartman, J. Behr, H. Izumi, D. Melconian, G. Morris, R. Nussbaumer, M. Olivo, M. Pearson, R. Poutissou, and G. Wight, Nucl. Instrum. Methods B **204**, 689 (2003).

[34] R. A. Cecil, B. D. Anderson, and R. Madey, Nucl. Instrum. Methods Phys. Res. **161**, 439 (1979).

[35] R. B. Firestone, *Table of Isotopes* (Wiley & Sons, New York, 1996).

[36] CERN Program Library.

[37] CERN Program Library entry D506.

[38] E. K. Warburton and B. A. Brown, Phys. Rev. C **46**, 923 (1992).

[39] B. A. Brown and W. D. Rae, http://www.nscl.msu.edu/~brown/resources/resources.html (2008).